

## Research Article

Nektarios Koukourakis\*, Robert Kuschmierz, Michael Bohling, Jürgen Jahns, Andreas Fischer and Jürgen W. Czarske

# Miniaturization of an interferometric distance sensor employing diffractive optics

**Abstract:** In order to improve safety, lifetime and energy efficiency of turbo machines, the behavior of the turbine blades has to be monitored during operation. This is a great challenge for metrology, since small, robust and non-contact position measurement techniques are required that offer both micrometer accuracy and micro-second temporal resolution. The Laser-Doppler-Distance (LDD) -Sensor proved to be an adequate technique to perform such measurements. However, the usage in turbo machines requires a miniaturized and temperature-stable sensor-head. In this paper we introduce a miniaturized design of the LDD-sensor that is based on common-path detection. First results indicated that the numerical aperture of the common-path detection is small in comparison to former implementations that used separate paths for illumination and detection. We find that decreasing the numerical aperture strongly increases the systematic measurement uncertainty. For this purpose a novel diffractive optical element containing a diffracting-lens was designed and used to increase the numerical aperture of the common-path detection without affecting the sensor size. Experiments prove that the new element reduces the relative systematic measurement uncertainty by a factor of ten. The mean systematic position measurement uncertainty amounts to  $\Delta z_{\text{mean}} \approx 16 \mu\text{m}$ . The resulting sensor has dimensions of  $25 \times 25 \times 60 \text{ mm}^3$ , offers temperature-stability and achieves micrometer resolution.

**Keywords:** diffractive elements; interferometry; Laser Doppler Sensor; miniaturization.

DOI 10.1515/aot-2014-0033

Received April 23, 2014; accepted June 27, 2014

## 1 Introduction

In-process measurements of position as well as dynamic deformations and vibrations of rotors in turbo machines are important tasks to optimize the rotor design and to validate numerical models of novel composite rotor designs [1]. Such measurements are a big challenge for metrology, as non-incremental and contactless measurement techniques are needed that provide high position resolution and concurrent high temporal resolution. Generally, optical techniques are advantageous over tactile methods as they operate contactless and offer high accuracy. However, the measurement rate of techniques like optical coherence tomography or confocal microscopy [2, 3] is limited by the speed of mechanical scanning or, in case of triangulation and digital holography, by the detector frame rate and minimum exposure time required [4–6]. Another drawback occurs when measuring rough surfaces because the coherent speckle noise fundamentally limits the measurement uncertainty of optical sensors [7]. Thus, highly dynamic measurements with  $\mu\text{m}$  precision of rotating rough objects which move at several hundreds of m/s are prohibited for most optical sensors.

A sensor based on Laser Doppler velocimetry was introduced that fulfills these requirements and enables measuring concurrently the tangential velocity and the radial position of rotating objects in a non-incremental manner [7–9]. The biggest advantage of this technique is that the measurement uncertainty is generally independent of the object speed. Hence, precise measurements even at high speeds over 600 m/s are feasible, as was already demonstrated in several model applications [10, 11]. These

---

\*Corresponding author: Nektarios Koukourakis, Laboratory for Measurement and Testing Techniques, TU Dresden, 01062 Dresden, Germany, e-mail: nektarios.koukourakis@tu-dresden.de  
Robert Kuschmierz, Andreas Fischer and Jürgen W. Czarske: Laboratory for Measurement and Testing Techniques, TU Dresden, 01062 Dresden, Germany  
Michael Bohling and Jürgen Jahns: Chair of Micro-and Nanophotonics, University Hagen, Universitätsstr. 27/PRG, D-58097 Hagen, Germany

unique properties of the sensor potentially open up applications in turbo machinery, e.g., for the realization of active clearance control systems, which could drastically improve the efficiency of turbo machines [10]. However, the sensor variants reported up to now were too bulky for the limited optical access present in turbo machines, because they used separate optical paths for illumination and detection. The required sensor for the usage in turbo machinery has a diameter in the range of 8–15 mm and has to be robust, which makes a lipstick-shape desirable. Furthermore, it has to potentially enable measurements at high ambient temperatures.

In this paper, we analyze the performance of a miniaturized LDD sensor-head that employs a common-path axial detection scheme. First measurements show that this implementation has a reduced numerical aperture, which leads to an increase of the systematic measurement uncertainty of the position. To improve the performance of the miniaturized sensor, a diffractive optical element is designed to increase the numerical aperture without changing the setup, as just one element is replaced. The performance of the improved miniaturized sensor is finally described.

## 2 Sensor principle

The LDD sensor is an extension of the conventional Laser-Doppler velocimeter. Instead of using one interference fringe system with constant spacing, the measurement volume of the LDD-sensor is created by two superimposed fan-shaped fringe-systems that have a fringe-spacing gradient along the axial direction [7]. Using a contrary orientation, i.e., one convergent and one divergent fringe system, introduces a position coding in axial direction. Separation of the two systems is achieved by wavelength division multiplexing.

With this setup, two Doppler frequencies from the two fringe systems can be measured simultaneously. The calibration function  $q$ , which is the quotient of the two Doppler frequencies  $f_{1,2}$  does not depend on the object velocity but just on the position (Equation 1).

$$q(z) = \frac{f_2(v, z)}{f_1(v, z)} = \frac{v(z)/d_2(z)}{v(z)/d_1(z)} = \frac{d_1(z)}{d_2(z)} \quad (1)$$

The relation between the axial position  $z$  and the calibration function  $q(z)$  can be expressed as:  $z = m^{-1} \cdot q + z_0$ , with  $m = \partial q / \partial z$  being the slope of the calibration function and  $z_0$  a constant. Hence, the axial position of an object crossing the measurement volume can be determined when the sensor

is properly calibrated. When the position  $z$  is known, the object velocity is accessible by using the local fringe spacing and applying the Doppler relationship  $v = d_1 \cdot f_1 = d_2 \cdot f_2$ . Hence, the LDD sensor enables simultaneously determining at which axial position  $z$  and with which transverse velocity  $v$  an object crosses the measurement volume.

## 3 Miniaturized sensor head

For measurements in turbo machines it is advantageous to create a modular setup which consists of an illumination unit, a detection unit and the passive optical sensor head, that are coupled with fibers. This approach allows separating the active optical elements from the rough ambient and proved to be beneficial in former investigations [7–11]. The illumination unit supplies the passive sensor head with two beams of different wavelengths using a single mode fiber. The sensor-head has to fulfill two tasks: First, it has to create the measurement volume. As the technique is interferometric the measurement head has to split the beams and overlap them in such a manner, that the two fan-shaped fringe systems are created. Second, the light scattered by the sample has to be coupled into a multi-mode fiber, which guides the light to the detection unit, where the signals are divided and detected separately for each wavelength. In former implementations of the sensor the illumination and the detection was implemented in separate arms [7–11]. Although these sensors were successfully used, the resulting setups were too bulky for some applications. In order to increase the applicability and pave the way for usage in turbo machinery, a further reduction of sensor size was necessary.

In this paper we propose a novel miniaturized design of the sensor head that applies a common-path setup for illumination and detection. An aspheric lens focuses the light of the single-mode fiber into the measurement volume. In order to minimize the number of optical elements in the sensor-head, the interferometer is implemented using diffractive elements [12]. A transmission-grating ( $g_1 = 4 \mu\text{m}$ ) located on a glass substrate in the beam path splits the light into different grating orders. While the zeroth and higher orders are blocked at the following element, the remaining four beams, i.e., the  $\pm 1$ st orders for each wavelength, pass a second transmission-grating ( $g_2 = g_3 = 3.3 \mu\text{m}$ ). These gratings create convergent beams that intersect in front of the sensor leading to interference patterns. The aspheric lens introduces dispersion, which is intentionally used to create longitudinally shifted beam waists for the two wavelengths. This shift is essential for the technique as it leads to the converging and a

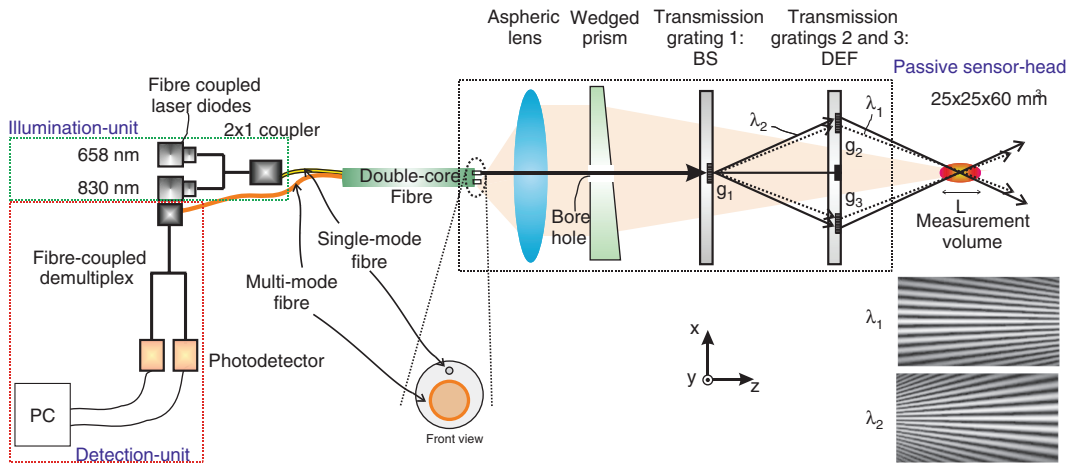


**Figure 1** Modular setup with miniaturized sensor-head.

BS is a  $1 \times 3$  beam-splitter and DEF is a deflection grating. The passive sensor-head creates the measurement volume which consists of two overlapping fan-shaped fringe-systems with contrary orientation, created at two different wavelengths.

diverging fan-shaped fringe system with contrary fringe spacing gradients (see Figure 1). In this initial configuration the measurement volume is located approximately 60 mm in front of the measurement head.

The most compact and robust detection design is to use the optical elements of the illumination also for the detection in a coaxial common-path scheme. Therefore a double-core fiber is employed, which bears the single-mode illumination core and a multi-mode detection core. The aspheric lens couples the backscattered light into the multi-mode core. To compensate for the lateral displacement of the cores, a wedged prism is located between the lens and the splitting grating. This prism has a bore-hole on the optical axis so that the illuminating-light passes without being affected. The detected light is then coupled into a fiber-based de-multiplexing unit which divides the two spectral components and allows for separate detection of two Doppler frequencies.

According to this concept, the size of the all-passive fiber-coupled sensor head can be miniaturized to dimensions of  $25 \times 25 \times 60 \text{ mm}^3$ . In contrast to former optical setups, all optical elements of the sensor-head can be manufactured of fused silica, which withstands temperatures up to  $1000^\circ\text{C}$ . Using sapphire fibers [13] for coupling the modular units and a temperature stable housing [11] could enable measurements at high-temperatures present in turbo-machines.

## 4 Experiments

At first, the calibration function  $q(z)$  of the sensor is determined. For this purpose a rotating disc containing a

pinhole is translated through the measurement volume of the sensor by a motorized stage. The disc is rotated with a stabilized known velocity. The light that propagates through the pinhole in axial forward direction is coupled into a separate multi-mode fiber. Thus, the calibration is performed with a separate detection path in order to gain precise knowledge of the fringe-systems, where errors due to the speckle-effect are excluded.

The two Doppler frequencies are measured and used to determine the fringe-spacing functions  $d_1(z)$  and  $d_2(z)$  of both fringe systems. To reduce the random errors, averaging over several roundtrips was used. The resulting calibration function  $q$  is shown in Figure 2 (left). It has a mean slope of about  $s=0.37 \text{ mm}^{-1}$ . The fringe spacings are plotted on the right of Figure 2. The different fringe-spacing gradients for the two wavelengths required for the LDD-sensor are clearly visible.

### 4.1 Measurement at rough surface with common path detection

The moving pinhole used for calibration creates a single point scattering, like the single particles that cross the measurement volume would do. At rough surfaces such as turbine blades, scattering will concurrently take place at multiple points located in the measurement volume. All individual scattering signals interfere at the photodetector resulting in time-varying speckle signal with a random envelope. The nature of the speckle pattern depends on the detection optics [14].

To analyse the performance of the common-path (CP) detection in comparison to separate-path (SP) detection,

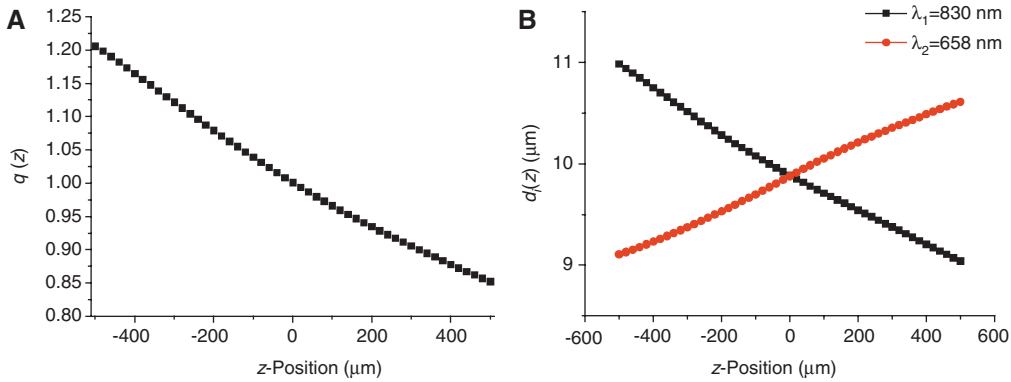
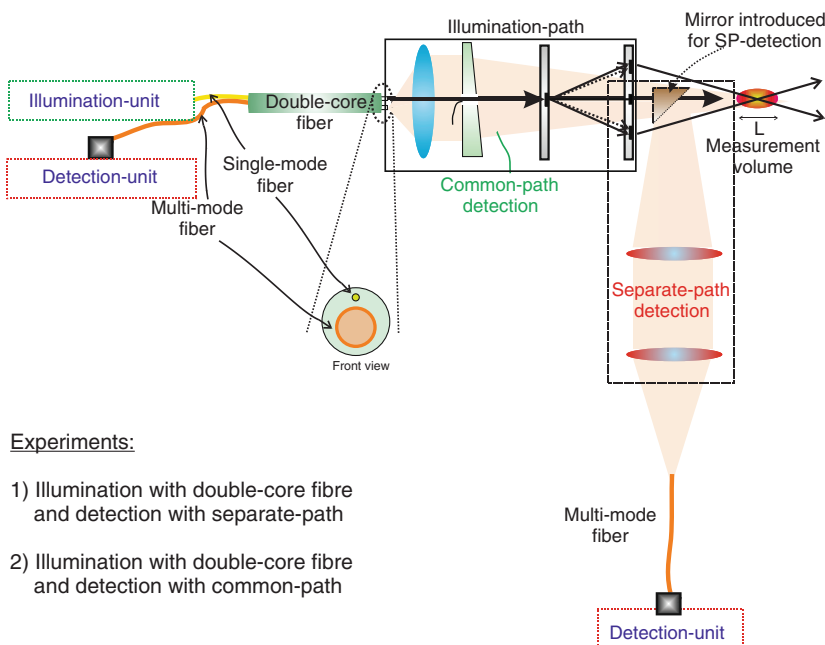


**Figure 2** (A) Measured calibration function  $q(z)$ . (B) Fringe-spacing along the z-axis.

the setup was implemented as sketched in Figure 3. We use the illumination-path of the miniaturized sensor to create the measurement volume. The setup allows using both CP- and SP-detection. For SP-detection a mirror is introduced, that deflects the scattered light towards the separate detection arm, where two lenses are used for coupling into the multi-mode fiber. For CP-detection, the mirror is removed and the scattered light is coupled into the multi-mode core of the double-core fiber. The measurements are performed sequentially, as the same detection unit is used for both detection architectures.

The test objects for the exemplary measurements were metal strip rotors with different degrees of surface roughness. The rotating sample was measured at several axial positions throughout the measurement volume and a function  $q_{\text{meas}}(z)$  was obtained. For the CP-detection the measured slope is decreased compared to the slope of the calibration function  $q(z)$  and amounts to  $s_{\text{meas,CP}} = 0.27 \text{ mm}^{-1}$  (Figure 4).

According to this measurement the fringe spacing seems to have changed. As the setup which is responsible for the fringe-properties is unchanged and the mean slope



#### Experiments:

- 1) Illumination with double-core fibre and detection with separate-path
- 2) Illumination with double-core fibre and detection with common-path

**Figure 3** Sketch of the used setup.

The single-mode core of the double-core fiber is used for illumination. Using the separate-path (SP)-detection and common-path (CP)-detection sequentially allows comparing the performance of both detection architectures.

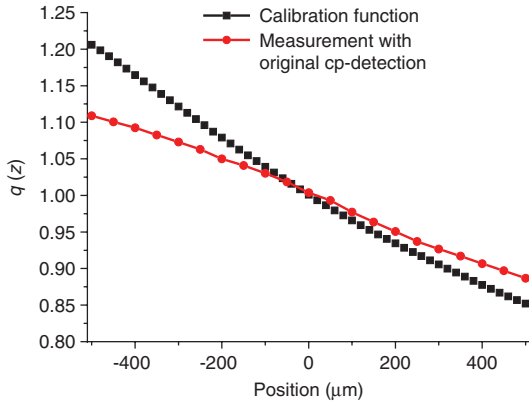


**Figure 4** The slope of the measured function  $q_{cp}$  for the common-path detection is strongly decreased in comparison to the calibration function.

for the measurement with separate path  $s_{meas,SP}=0.36 \text{ mm}^{-1}$  is comparable to the slope of the calibration function, this phenomenon can only be introduced by the different detection architectures.

Analysing the differences between the SP and CP-detection, we find that the common-path detection has a relatively low numerical aperture of  $NA_{CP}\approx 0.02$ , which is considerably smaller than the numerical aperture for common setups that use separate detection arms of  $NA_{SP}\approx 0.1$ . The reduced NA leads to an increase of the speckle size, which reduces the speckle number used for signal formation. The consequence of the changed speckle-effect is a spectral broadening of the Doppler-peaks, which shifts the peak frequencies and thus directly affects the slope of the calibration function. A comparable dependence between speckle-number and spectral broadening of the Doppler-peak was observed in a Laser-Doppler velocimeter [15].

Consequently, the change of the speckle-properties changes the slope of  $q$ , which results in a strong deviation of the measured position to the default position  $\Delta z$ . This corresponds to an increase of the systematic measurement uncertainty, which is inhomogeneous across the measurement volume. At the borders of the measurement volume the maximum deviation for the common-path detection reaches  $\Delta z_{max,CP}\approx 225 \mu\text{m}$ . The described behavior was observed for all measured surfaces, while the exact degree of slope-change and the consequent systematic error  $\Delta z$  depend on the speckle-path used. For detection with separate-path, the maximum deviation is  $\Delta z_{max,SP}\approx 13 \mu\text{m}$  which is comparable to the experiences with other setups.

The random errors of the position measurement are obtained by the standard deviation of consecutively repeated measurements. The mean random error of the

position across the measurement volume for the common-path detection amounts to  $\sigma_{z,mean}\approx 3.75 \mu\text{m}$ . It is nearly homogeneous across the measurement volume and just increases at the borders, as here the intensity is decreased compared to the center. The mean random uncertainty for the common-path detection is about three times larger than for separate detection. This is due to the reduced collection efficiency of the common-path detection, which results in a drop of the SNR by a factor of  $\sim 10$ . Hence, there is no evidence of an influence of the speckle-effect on the statistical measurement uncertainty.

The results presented in this section prove that the illumination-path of the miniaturized sensor-head works adequately, as the separate-path detection shows an expected performance. The common-path detection instead suffers of a reduced numerical aperture, which enforces strong improvement, to enable the aimed high-quality measurements. For this purpose, the numerical aperture of detection has to be increased to reduce the systematic uncertainty. In order to keep the advantage of the miniaturized setup, this has to be achieved without any increase of sensor size. Two approaches are discussed in the next section.

## 5 Improved common-path detection employing diffractive optics

The numerical aperture of the common-path detection design is low, as the distance between the measurement volume and the aspheric lens that couples the scattered light into the multi-mode core is large. We use two approaches to increase the NA.

### 5.1 Reduction of working distance

As a first step of improvement, the measurement volume is moved closer to the measurement head by replacing the diffracting transmission grating 1 with  $g_1=4 \mu\text{m}$  by another grating of  $g_1^*=5 \mu\text{m}$ . This change has influence; First, as purposed the measurement volume is created at a halved distance  $d=30 \text{ mm}$ . As a result, the detection NA is increased from  $NA_{CP1}=0.02$  to  $NA_{CP2}=0.03$ . Second, the change leads to an increased intersection angle, which decreases the axial extent of the measurement volume to about  $600 \mu\text{m}$  and changes the fringe-number and also the fringe-spacing. The resulting value for the maximum deviation is  $\Delta z_{max,with g^*}\approx 30 \mu\text{m}$ .

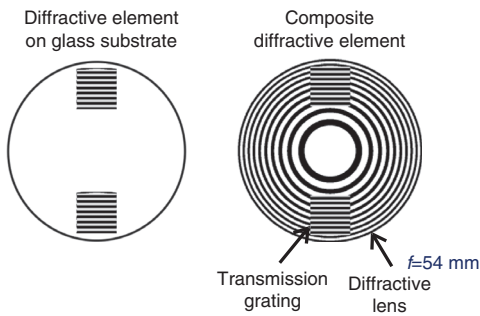


**Figure 5** The simple DEF transmission grating (left) is replaced by the composite diffractive element containing the transmission grating and a diffractive lens (right).

The length of the measurement volume is different than before we introduce the relative systematic uncertainty, which is given by the quotient of the maximum position deviation  $\Delta z_{\max}$  to the length of the measurement volume. The grating change improved the relative deviation by a factor of 4.5. Hence, the shift of the measurement volume closer to the sensor successfully decreased the systematic uncertainty and showed that a further improvement of NA would be beneficial.

## 5.2 Increased NA by using a diffractive lens

A novel composite diffractive optical element (DOE) was designed and fabricated by standard mask-based lithography [16], to replace the DEF transmission gratings (Figure 1). It consists of a diffractive lens which was implemented with three discrete phase levels. The diffractive

lens also contains two inserted gratings that are used to replace gratings  $g_2$  and  $g_3$ . Thus, the introduction of this DOE-element does not change the illumination-path and the setup-size is kept constant. The diffractive lens is used to collimate the scattered light and thus to increase the light-collecting efficiency of the common-path detection. Its focal length is  $f=54$  mm. The introduction of the novel DOE-element readjust the axial position of the wedged prism to compensate for changes of the image position. The deflecting element and the novel DOE composite element are depicted in Figure 5. Using the diffracting element the numerical aperture is improved by a factor of about 3.5 to 0.07. At this time, we did not aim particularly at high performance. Parameters like NA and efficiency might still be improved with a further improved design.

In the following experiment the configuration with the grating  $g_1=4$   $\mu\text{m}$  was used again. Using the CP-detection with DOE, the maximum deviation amounts to  $\Delta z_{\max, \text{DOE}} \approx 21$   $\mu\text{m}$ . The systematic measurement uncertainty of the position is homogeneous across the measurement volume and just slightly higher than for the separate-path detection (Figure 6A). An increased uncertainty noise for CP-detection is observable in Figure 6A. This can be attributed to the difference of speckle-size and speckle-number used for signal-formation and to spurious reflections from surfaces across the optical path that are coupled into the detection fiber and lead to interference effects. The incorporation of the novel diffractive element decreased the relative systematic uncertainty by a factor of 10 compared to the original common-path detection due to the improved NA. With this setup the mean systematic measurement uncertainty amounts to  $\Delta z_{\text{mean, DOE}} \approx 16$   $\mu\text{m}$ . The random

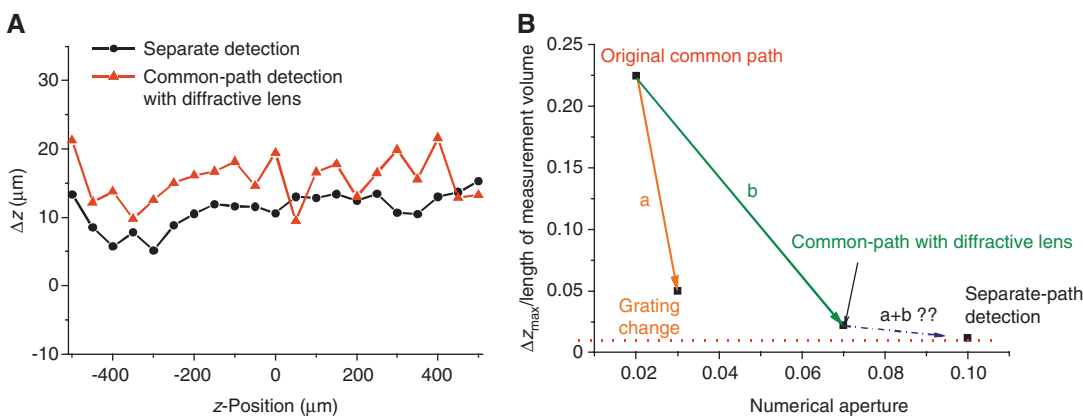


**Figure 6** (A) Systematic measurement uncertainty for the position. As a result, the incorporation of the diffractive lens enabled to miniaturize the LDD-sensor and to achieve a sensor-performance comparable to the sensor with separate detection. (B) The relative systematic measurement uncertainty for all tested detection architectures. The common-path implementation with DOE nears the performance of the separate-path detection. A combination of the approaches A and B promises further improvement.

errors are also decreased to a mean value of  $\sigma_{z, \text{mean}} \approx 2.1 \mu\text{m}$ , as the improved NA is accompanied by a four-fold increase of the light-collecting efficiency of the sensor.

Figure 6A shows a summary of the relative systematic measurement errors for all tested configurations. The performance of the common-path detection with DOE nears the performance of the setup with separate detection path. Further improvement can be achieved, when approaches A and B are combined, i.e., the common-path detection is implemented with DOE and the changed grating configuration that shifts the measurement volume closer to the sensor head. For this purpose an adjusted focal length of the DOE element is required.

## 6 Conclusion

In this paper we investigate a concept for miniaturization of a Laser-Doppler-Distance-sensor with common-path detection. We find that the simple change of the setup to common-path detection is accompanied by a reduced numerical aperture, which leads to an increase of the systematic measurement uncertainty due to the speckle-effect. As the reduction of NA decreases the SNR, also the random measurement uncertainty increases.

We proposed two approaches to compensate for these effects, that both proved to be beneficial. First, the measurement volume was moved close to the sensor head using a changed grating configuration. This led to an increase of the NA and to strong reduction of the systematic measurement uncertainty. For the second approach, the DEF element on simple glass-substrate was replaced by a novel composite diffractive optical element incorporating a diffractive lens. This change increases the NA for the common-path detection by a factor of 3.5.

The increased NA led to a decrease of both the random and the systematic measurement uncertainty. The relative systematic measurement uncertainty is improved by a factor of 10, with the the mean systematic measurement uncertainty amounting to  $\Delta z_{\text{mean}} \approx 16 \mu\text{m}$ . The random errors are decreased to a mean value of  $\sigma_{z, \text{mean}} \approx 2.1 \mu\text{m}$  as the improved NA is accompanied by a four-fold increase of the light-collecting efficiency of the sensor.

Most importantly, these improvements are achieved without increasing the sensor size. Despite the miniaturization of the sensor, the gap between the performance of a separate detection arm and the common-path detection diminished by the usage of the novel composite diffractive

element and could be completely closed with further optimization of the used elements, for example using a combination of the two presented approaches.

The achieved size of the miniaturized sensor is  $25 \times 25 \times 60 \text{ mm}^3$ . All optical elements used can be made of fused silica, so that the sensor potentially offers high-temperature stability up to  $1000^\circ\text{C}$ . To compensate for thermal expansion the setup could be implemented in a temperature stable housing introduced in [10]. The presented results can be seen as a first step towards the miniaturized sensor required for in-process measurements at turbo-machines, which could e.g., allow for tip-clearance control.

**Acknowledgments:** The authors thank the Deutsche Forschungsgemeinschaft (DFG) for their financial support (project Cz 55/23-1). We also acknowledge the work of Thomas E. Seiler and Boguslaw Wdowiak, University of Hagen.

## References

- [1] R. Kuschmierz, A. Filippatos, A. Langkamp, W. Hufenbach, J. W. Czarske, et al., SPIE Proc. 906200-906200-7 (2014).
- [2] D. Huang, E. A. Swanson, C. P. Lin, J. S. Schuman, W. G. Stinson, et al., Science 254, 1178–1181 (1991).
- [3] R. H. Webb, Rep. Prog. Phys. 59, 427–471 (1996).
- [4] R. G. Dorsch, G. Häusler and J. M. Herrmann, Appl. Opt. 337, 1306–1314 (1994).
- [5] A. Kempe, S. Schlamp, T. Rösger and K. Haffner, Opt. Lett. 28, 1323–1325 (2003).
- [6] Y. W. Lai, N. Koukourakis, N. C. Gerhardt, M. R. Hofmann, R. Meyer, et al., J. Microelectromechanical Sys. 19, 1175–1179 (2010).
- [7] T. Pfister, L. Büttner and J. Czarske, Meas. Sci. Tech. 16, 627–641 (2005).
- [8] F. Dreier, P. Günther, T. Pfister, J. Czarske, A. Fischer, IEEE T. Instrum. Meas. 62, 8 (2013).
- [9] P. Günther, F. Dreier, T. Pfister, J. Czarske, T. Haupt, et al., Meas. Syst. A. Sig. Proc. 25, 319–330 (2011).
- [10] T. Pfister, P. Günther, F. Dreier, J. Czarske, J. Eng. Gas Turb. Power 134, 012504-1–012504-7, (2011).
- [11] F. Dreier, T. Pfister and J. Czarske, Proc. Of ASME Turbo Expo in Copenhagen, Denmark. GT2012-69540 (2012).
- [12] J. Schmidt, R. Völkel, W. Stork, J.T. Sheridan, J. Schwider, et al., Opt. Lett. 17, 1240–1242 (1992).
- [13] Y. Zhu, Z. Huang, F. Shen and A. Wang, Opt. Lett. 30, 711–713 (2005).
- [14] J. W. Goodman, JOSA 66, 11, 1145–1150 (1976).
- [15] R. Kliese and A. D. Rakic, Opt. Express 20, 18757–18771 (2012).
- [16] J. Jahns, S. Helfert, 'Introduction to Micro- and Nanooptics', Wiley VCH Weinheim ch.6 (2012).



Nektarios Koukourakis studied electrical engineering at the Ruhr-University in Bochum, Germany. He received his diploma degree in 2008 and his PhD degree in 2012. Since 2013 he is with the Laboratory for Measurement and Testing Techniques at the Technische Universität, Dresden. His current research areas are the development of novel optical measurement systems for surface analysis and biomedicine, based on interferometry, holography and novel microscopic approaches.



Robert Kuschmierz received his diploma degree in electrical engineering in 2012 from the Technische Universität Dresden, Germany. Since 2012, he is working in the group of measurement system techniques at the Laboratory for Measurement and Testing Techniques. His main research areas are the development, characterization and application of laser-based measurement systems for shape and vibration measurements in production engineering as well as in non-destructive testing for turbo machinery.



Michael Bohling received his Diploma degree in applied physics from the University of Applied Sciences in Emden, Germany, in 1988, and his MSc degree in photonics from the University of Hagen, Germany. In 2012 he received his PhD degree in electrical engineering from the University of Hagen. Between 1990 and 2003 he was with several laser material processing companies, eventually in the position of CEO. He is currently a research assistant in the Micro- and Nanophotonics group with the University of Hagen.



Jürgen Jahns received his diploma and doctorate in physics from the University of Erlangen-Nuremberg, Germany, in 1978 and 1982, respectively. He worked at Siemens, Munich, Germany, and at AT&T Bell Laboratories, Holmdel, New Jersey, before becoming Full Professor and Chair of Optical Information Technology at the FernUniversität in Hagen, Germany, in 1994 (now: Chair of Micro- and Nanophotonics). He has co-authored more than 95 journal articles and several books on microoptics and photonics. Jahns is a Fellow of OSA and SPIE and a member of DGaO, EOS, and IEEE.



Jürgen Czarske studied electrical engineering and physics at the Universität Hannover, where he received his PhD in 1995 and the *venia legendi* in 2003. Between 1995 and 2004, he was with the Laser Zentrum Hannover e.V. and, since 2004, he has been Professor for Measurement and Testing Techniques at the Technische Universität Dresden. His current research activities focus on developing novel optical and ultrasonic sensors for investigating fluid flows as well as the dynamic behavior of solid objects.



Andreas Fischer received his diploma degree in electrical engineering in 2004 and his PhD degree in 2009 from the Technische Universität Dresden, Germany. Since 2009, he is the head of the group of measurement system techniques at the Laboratory for Measurement and Testing Techniques. His main research areas are the identification, characterization and application of measurement limits as well as the development of optical flow and surface measurement systems.